

LIBRARY
282
MET. O.14

METEOROLOGICAL OFFICE
BOUNDARY LAYER RESEARCH BRANCH
TURBULENCE & DIFFUSION NOTE



143304

T.D.N. No. 155

A COMPARISON OF SEVERAL METHODS OF ASSESSING
THE SURFACE ENERGY BALANCE OVER A GRASS SURFACE

- A preliminary report on the Cardington experiment, 1983

by

WANG JIEMIN*

The Institute of Plateau Atmospheric Physics

Chinese Academy of Sciences

Lanzhou, China

May 1984

*This work was carried out at the Boundary Layer Research Branch,
Meteorological Office, UK.

Please note: Permission to quote from this unpublished note should be
obtained from the Head of Met.O.14, Bracknell, Berks, U.K.

FH5B

A comparison of several methods of assessing the surface energy balance over a grass surface - A preliminary report on the Cardington experiment, 1983

1. Introduction

From 21 April to 18 May, 1983, an experiment was carried out at the Meteorological Research Unit, RAF, Cardington, to measure directly the components of the energy budget over a grass surface. The principal objective of the experiment was to verify the model, developed mainly from the Cardington data, 1976, for estimating the heat and momentum fluxes in the surface layer from routine meteorological data (Smith and Hunt, 1978; Wang, 1984). Further instrumentation was set up to enable independent estimates of the fluxes to be made for intercomparison. The weather during the observational period was very changeable and mostly rather wet. The daily rainfall during this period is shown in Fig. 1.

The data (hourly mean values) are presented in the Appendix; they were selected according to the following criteria:

- a. No rainfall during the hour of observation;
- b. No identifiable instrument malfunction.

2. Site description

The experimental area is illustrated in Fig. 2 which shows the distance and bearing of the nearest obstacles to the 16 m profile mast. It provides a good exposure to the wind from most directions. There are, however, two large hangars (approximately 50 m high) about 300 m to the north. The laboratory buildings (approximately 4 m high) 50 m to the east of the two 16 m masts may have more influence on the profile measurements. Other buildings and topographic changes normally lie 1-2 km away. The most open area lies in south-west (190° - 300°).

Both the site and its immediate surroundings are grass covered. The grass height was normally about 10 cm; but late in the observational period the grass in the instrumented area grew up to 20-25 cm.

3. Measurement of the surface energy budget

The measurement of the surface energy budget was done in four ways:-

- a. Direct measurement of net radiation, evaporation and soil heat flux and the use of an energy balance equation to derive the sensible heat flux;
- b. Estimation of fluxes from mean wind and temperature profiles;
- c. Direct measurements of sensible heat and momentum fluxes by sonic anemometer;

d. Routine meteorological observations.

These measurements are described below.

i. Net radiation

The net radiation R_n was measured by two types of net radiometer: one is a standard polythene-shielded Funk type; the other is a ventilated Kew Observatory pattern. Both were supported parallel to the surface at a height of approximately 1 m. The accuracy is between 5 and 10 percent. The readings of the two radiometers agree very well, except during precipitation when the Kew type was apparently unreliable.

ii. Evaporation

Evaporation was measured directly by a lysimeter, a square tank of surface area 2 m^2 and depth 50 cm, containing a sample of soil and a grass surface representative of the surrounding site. The tank is mounted on a balance constructed in situ around it. The change in the weight of this tank due to evaporation from the surface or rainfall upon it is monitored automatically. If $\Delta h \text{ mm}$ is the equivalent depth of water evaporated from the surface of the lysimeter during a period Δt seconds, the rate of evaporation E per unit area is given by

$$E = \frac{\Delta h}{\Delta t} \text{ kg.s}^{-1}\text{m}^{-2} \quad (1)$$

The latent heat flux

$$LE = \lambda E \quad (2)$$

where λ is the latent heat of water vaporization.

The lysimeter cannot normally resolve variations in the evaporation rate over periods less than one hour. This is due to the difficulty of monitoring the small weight change of the huge amount of soil, and also, due to the effect of the turbulent wind field over the surface of the lysimeter. During the experiment the output of the lysimeter often appeared to have an oscillation with period approximately 3 min, which might be one of the resonant oscillations of the mechanical system of the balance. But, nevertheless, the lysimeter has proved to be a direct and consistently reliable means of presenting an hourly mean value of LE continuously, with an accuracy of between 10 and 20 percent.

iii. Soil heat flux

Three conventional flux plates were buried at depths of 5, 10 and 15 cm under the surface to measure the heat flux at those depths. The downward soil heat flux G at the surface ($Z=0$) is estimated by extrapolation from the outputs of the three plates. This is because it is physically impossible to measure this quantity without disturbing the surface. Furthermore, not only does the finite size of

the sensors produce an unavoidable volume - integrated measurement, but also the sensors must be buried deep enough to prevent any direct sky or solar radiation reaching them.

The diurnal variation of soil heat flux in a two-day period is shown in Fig. 3. It is very similar to Richards' result which was obtained from the 1976 experiment at Cardington (Richards, 1979). Again, Richards' extrapolation table for deriving G has proved to be adequate for processing the data from the flux plates used in this experiment.

iv. Sensible heat flux

The sensible heat flux H can be calculated from the well known surface energy balance equation

$$R_n = H + LE + G \quad (3)$$

after we have obtained the values of R_n , G, and LE from the measurements mentioned above. This is the residual method. Other methods of obtaining H will be given later.

v. Wind and temperature profiles.

A 16 m mast was used with a wind vane at the top and 4 Porton-type anemometers mounted at 1, 3, 8.7 and 16 m to measure the wind profile. Temperature differences were measured between 0.5 m and 2 m and between 0.5 m and 8 m using three thermistors with radiation shielding and natural aspiration.

The use of profile data to evaluate fluxes and the comparison with other methods are discussed in section 4.

vi. Direct measurements of turbulent fluxes

A sonic anemometer mounted at the top of a 16 m mast was used to measure the turbulent fluxes directly. A fast temperature sensor consisting of a 0.025 mm platinum wire was attached to the sonic head, and the output processed with the sonic signals. By this means more precise measurements of mean temperature (t_p) and sensible heat flux (H_p) can be obtained.

The sonic anemometer worked very well through the whole observational period. Unfortunately the attached platinum wire is very fragile and broke at some time during the last 9 days.

vii. Standard meteorological observations

Observations of screen dry-and wet-bulb temperatures were made when possible, and a thermograph and hygrograph provided values of temperature and relative humidity during periods when no observer was present. The accuracies of the thermograph and hygrograph were poor, so observations from RAE Bedford were used as a check in the later data analysis.

A sky camera was used to take pictures of cloud cover normally once an hour. The cloud data from Bedford station were used as a check as well.

A raingauge was used to measure the amount and time period of rainfall.

4. Analysis of the data

a. Diurnal variation of the wind profile and surface energy budget.

In Fig. 4 the hourly variation of the wind profile is shown for two rather fine days with a wind direction (at 16 m) mainly SSW. It illustrates the classical departure of the vertical wind profile from the logarithmic law in diabatic conditions. When the layer is unstable, e.g. around midday, the profile is curved towards "Height"

axis. However when the layer becomes rather stable the curvature reverses its sense. This behaviour is predictable from the similarity theory shown by equations (6) and (9) in the next paragraph.

Fig. 5 shows the hourly variation of the components of surface energy budget for the first four days, which are representative of the whole observational period. Of the four terms in the budget it is noted that the net radiation R_n is generally the largest, and, furthermore, is usually subject to the greatest daily changes. This is because R_n is strongly dependent on the elevation of the sun and on meteorological factors such as cloud cover (type, amount and depth), and atmosphere turbidity. We have developed a model to evaluate R_n based on these factors, which will be discussed later. The other components in the energy budget reflect the variation in R_n to a greater or lesser degree. Soil heat flux G , for instance, follows R_n closely, but with greatly reduced amplitude. Smith's formula,

$$G = \left(0.4 \frac{S}{S_m} - 0.2\right) R_n \quad (4)$$

(F B Smith, Private communication) is suitable for use in modelling work, where S is solar elevation (see later, equation (23)), and S_m is the midday value of S .

The latent heat flux LE plays a very important role in the surface energy budget. In this observational period, LE is the second largest term, and is a strong function of R_n . This is because there is an adequate supply of soil moisture in this period. Generally LE is a

complex function of R_n , G , the drying power of the wind (i.e. wind speed and relative humidity), and the ground state, mainly the moisture content of the soil. Monteith presented a formula to estimate LE by introducing the surface resistance (Monteith, 1965), which will be discussed in the last part of this section.

b. Analysis of the profile data.

Based on the Monin-Obukhov similarity theory for the surface layer of the atmosphere boundary layer the so-called profile method was used to estimate the heat and momentum flux at the surface. According to the similarity theory, with the assumption of stationary and horizontally homogeneous conditions, vertical gradients of any conservative quantity are functions of height Z and Z/L only, where

$$L = - \frac{\bar{\theta} u_*^3}{g k H} \rho C_p \quad (5)$$

is the Monin-Obukhov length; u_* , the friction velocity; $\bar{\theta}$, the mean potential temperature of the surface layer; K , the Von Karman constant; ρ , the density of air; C_p , the specific heat of air at constant pressure. For wind and temperature we have

$$u(z_2) - u(z_1) = \frac{u_*}{K} \cdot \psi_m \quad (6)$$

$$\theta(z_2) - \theta(z_1) = - \frac{\theta_*}{K} \cdot \psi_h \quad (7)$$

where Z_1 and Z_2 are two heights at which wind and temperature are measured, θ_* is a scaling quantity defined by

$$H = \rho C_p u_* \theta_* \quad (8)$$

γ_m and γ_h are the so-called integrated universal functions (Paulsen, 1970):

Unstable case ($Z/L < 0$)

$$\gamma_m = \ln \frac{Z_2}{Z_1} + \ln \left[\frac{(X_1^2+1)(X_1+1)^2}{(X_2^2+1)(X_2+1)^2} \right] + 2(\tan^{-1} X_1 - \tan^{-1} X_2) \quad (9)$$

$$\gamma_h = \alpha \left[\ln \frac{Z_2}{Z_1} + 2 \ln \left(\frac{Y_1+1}{Y_2+1} \right) \right] \quad (10)$$

Stable case ($Z/L > 0$)

$$\gamma_m = \ln \frac{Z_2}{Z_1} + \frac{\beta}{L} (Z_2 - Z_1) \quad (11)$$

$$\gamma_h = \alpha \ln \frac{Z_2}{Z_1} + \frac{\beta}{L} (Z_2 - Z_1) \quad (12)$$

where

$$X_1 = \left(1 - \gamma_m \frac{Z_1}{L} \right)^{1/4} \quad (13)$$

$$X_2 = \left(1 - \gamma_m \frac{Z_2}{L} \right)^{1/4} \quad (14)$$

$$Y_1 = \left(1 - \gamma_h \frac{Z_1}{L} \right)^{1/2} \quad (15)$$

$$\gamma_2 = \left(1 - \gamma_h \frac{z_2}{L}\right)^{1/2} \quad (16)$$

There are at present two widely used parameterizations

a. $\gamma_m = 15, \gamma_h = 9, \alpha = 0.74, \beta = 4.7, K=0.35$ (17)
 (Businger et al, 1971)

b. $\gamma_m = \gamma_h = 16, \alpha = 1, \beta=5.0, K=0.40$ (18)
 (Dyer and Hicks, 1970)

Equations (6) - (8) were used to calculate u_* and H from the profile data. The accuracy of the results is clearly limited by the semi-empirical description of γ_m and γ_h . For Cardington data, furthermore, it is noticed that because the profile mast is surrounded by buildings and other topographic features, the surface layer, in which the vertical variation of the fluxes is very small (e.g. less than 20%), is rather shallow. So for the comparison with other surface measurements only the lowest layer of the profile data was used in the calculation.

Fig. 6 shows a comparison of sensible heat flux calculated by the profile method and by the residual method (Eq. (3)). It is not surprising that the points are rather widely scattered due to the errors of measurements in both methods. However, the correlation between the two sets of result is very good.

The values of H and U_* from the profile method were compared with those directly measured by the sonic anemometer. These are shown in Fig. 7 and 8. The values of sensible heat flux measured by sonic anemometer are rather lower, particularly in the daytime when H is rather large. This is very likely due to the height difference - as mentioned above, the sonic anemometer was mounted at 16 m, but the data used in the profile method are from the lowest layer (0.5 - 3 m) only. It may have been better to mount the sonic anemometer at a lower height in this experiment.

The Dyer and Hicks' parameterization (18) was used in the profile method calculation mentioned above. The difference between the results obtained by use of Dyer and Hicks' scheme and Businger et al's scheme is normally less than 5%.

c. Roughness length

Roughness length Z_0 is one of the most important parameters in modelling the boundary layer. In neutral conditions it can be evaluated by use of the logarithmic law,

$$\frac{ku}{u_*} = \ln \frac{z}{Z_0} \quad (19)$$

Then

$$\ln z = \frac{k}{u_*} u + \ln Z_0 \quad (20)$$

where u is the wind speed at height z . Equation (20) can be used to determine Z_0 from the wind profile measurements by linear regression of u on z , i.e. no independent evaluation of U_* and K is required. The slope of the regression line of course gives K/U_* .

In the absence of truly neutral runs, as in our case, the determination of Z_0 is not so straightforward. Here the 'profile method' outlined in last paragraph was used. For unstable conditions, from the wind profile of the integrated form (6).

$$\frac{ku}{U_*} = \ln \frac{z}{Z_0} + \ln \left[\frac{(x^2+1)(x_0+1)^2}{(x^2+1)(x+1)^2} \right] + 2\tan^{-1}x - 2\tan^{-1}x_0$$

$$\approx \ln \frac{z}{Z_0} - \ln \left[\left(\frac{x^2+1}{2} \right) \left(\frac{x+1}{2} \right)^2 \right] + 2\tan^{-1}x - \frac{\pi}{2} \quad (21)$$

where $x = (1 - 16 \frac{z}{L})^{1/4}$, $x_0 = (1 - 16 \frac{Z_0}{L})^{1/4}$ (using Dyer and Hicks' scheme). In this experiment, normally, $|L| > 10m$. So it is adequate to assume $x_0 = 1$ to simplify the calculation.

Z_0 was calculated for each wind profile measurement in the unstable case, by use of (21). The results are shown in Fig. 9 and 10.

Fig. 9 shows Z_0 as a function of wind direction, for each half of the observation period. The mean value in the second half period is larger than that of the first half period because the grass had grown. The effect of wind direction is also seen, particularly in Fig. 10, in which estimates of Z_0 have been made from the wind shear over different height intervals. The values of Z_0 calculated from the

wind speeds at 8.7 and 16 m are apparently greater with winds from 90° - 120° , as in Fig. 9. This reflects the influence of the laboratory buildings which are only 50 m away to the east of the profile mast.

d. The relationship between net radiation and solar elevation for different cloud conditions.

The net radiation R_n plays a predominant role in the surface energy balance. Its estimation from readily available meteorological data, i.e. solar elevation and cloud cover, has been discussed by many authors (e.g. see Nielsen et al, 1981). Based on the analysis of Cardington data (1976), we have developed a model (Wang, 1984) which is efficient and convenient for practical use. According to the model, R_n can be evaluated by following equation:

$$R_n = a_0 + a_1 s + a_2 s^2 + a_3 s^3 \quad (22)$$

where s is solar elevation (the sine of solar elevation angle), which is related to the latitude ϕ of the station, the Julian day number n and the local time t :

$$s = \sin\phi \sin A + \cos\phi \cos A \cos \frac{\pi}{12} (t - 12) \quad (23)$$

where

$$A = 23.3 \sin \left[\frac{2\pi(n-81)}{N} \right] \quad (24)$$

N is the number of days in the year (365 or 366). The coefficients a_0-a_3 in (22) are mainly related to the cloud cover and must be determined empirically. In our model, for a short grass surface, the coefficients are shown in the following Table.

Cloud condition	a_0	a_1	a_2	a_3
I	-45.0	102.5	742.2	-172.1
II	6.2	41.6	155.9	99.6

Unit: W/m^2

The cloud cover has been very much simplified by grouping into only two classes. The "total amount" refers to medium and low cloud only, high cloud being neglected.

- I. total amount ≤ 6 oktas,
- II. Total amount ≥ 7 OKTAS.

Fig. 11 shows the variation of R_n in a typical partly cloudy day (condition I) in this experiment. The observed hourly mean value and the value calculated by the model are also plotted. It can be seen that even though the value of R_n fluctuated a good deal because of the very changeable cloud state, the model value is still a good representation of the hourly mean value.

Fig. 12 and 13 show the comparison between the observed value and the model value of R_n for the whole period of this experiment. Since the weather in this period was very changeable, the points are rather scattered. But the agreement is still very good.

e. Estimation of surface turbulent fluxes from routine meteorological data.

The model for this estimation has been fully discussed by Wang (1984). Briefly, this model consists of a set of empirical formulae to evaluate the parameters in the Monteith Formula (Monteith, 1965).

$$H = \frac{r_a + r_{st} - r_i}{(1 + \bar{\Delta}/\gamma)r_a + r_{st}} (R_n - G) \quad (25)$$

After the estimation of H , U_* can be calculated from the similarity equations, such as (6), (9) etc., and by use of a method of interactive calculations.

In equations (25), r_a , r_{st} and r_i are the so called resistances of the surface layers. r_a is mainly related to the wind speed,

$$r_a \approx 260/u_{10} \quad (26)$$

where U_{10} is the wind speed at a standard height 10 m. r_i is mainly related to the humidity of the air,

$$r_i = \frac{\rho C_p}{\gamma(R_n - G)} \varrho_s(T) \left(1 - \frac{h}{100}\right) \quad (27)$$

where h is the relative humidity observed at screen level, $\ell_s(T)$ is the saturated water vapour pressure at the observed screen temperature T , and $\gamma = 0.646$ is the so called psychrometric parameter.

r_{st} , the so called stomatal resistance, was introduced by Monteith (1965) to relate the latent heat flux, i.e. the evaporation from the vegetated ground, with the micrometeorological state just within the vegetated surface. r_{st} is small when there is more water available in the ground; r_{st} is large when the ground is dry and the temperature is high. Many authors (e.g. Deheer et al, 1981) have tried to evaluate r_{st} using standard meteorological data. The new model (Wang, 1984) under consideration here is convenient in use, and is mainly based on the following considerations:

i. r_{st} during the few hours directly after rainfall is very small ($0-50 \text{ sm}^{-1}$).

ii. After an appreciable rainfall (daily amount $\geq 1 \text{ mm}$), the value of r_{st} drops down to a minimum value at first, then it increases day by day, the rate of increase being larger when the daily mean temperature is higher. During a hot/dry spell, after 10 days, r_{st} may be as large as $1000-2000 \text{ sm}^{-1}$.

iii. For a more reliable estimation, the hourly variation of r_{st} during the day should be considered. In the early morning, particularly when there is a dewfall, r_{st} is normally less than

50 sm^{-1} ; then, it increases with time till about 09 hours local time. From about 09 to about 17 hours, r_{st} is nearly a constant at the daily mean value as estimated by ii. In the late afternoon, for a few hours, r_{st} may reach a peak value and then decrease rapidly during the evening.

The results derived from this model (the so-called resistance method) for the period of this experiment are compared with those from the profile method in Fig. 14. Fig. 15 shows a comparison of friction velocity U_* derived from the two methods. A iterative calculation has been used in deriving U_* in the resistance method. It can be seen that the agreement between the two methods is very good.

5. Concluding remarks

From the data analysis, the following remarks can be made:

- a. The experiment was generally successful. Although the weather in the observation period was rather wet and changeable, causing malfunction of some instruments at times, most of the data (over 400 hours) are still reliable. Compared with the 1976 experiment (Richards, 1979), this was a short period of observation. However since the main intention was to carry out a careful investigation of the surface energy balance, many of the measurements were specially made and every effort was made to ensure that the data were reliable.

b. Our model for estimating net radiation R_n and sensible heat flux H (and friction velocity U^*) from readily available meteorological data was based on the analysis of data from the 1976 experiment at Cardington. Some parts of the model were slightly modified to provide a better fit to the data from both experiments. It was shown in last section that the model is adequate. This gives us more confidence to use the model to treat some independent data sets. The result is satisfactory (Wang, 1984).

c. The four methods of measuring or estimating the surface fluxes, namely the residual method, the profile methods, the resistance method, and the eddy-correlation method (through turbulence measurements), are proved to be compatible in this experiment. The fluxes measured by sonic anemometer were slightly lower than the result of other methods. It is very likely because of the rather shallow surface layer at Cardington.

d. The data are worth further investigation and could be useful for other studies. For this reason the hourly mean values of the data are tabulated in the Appendix.

Acknowledgement

The author would like to express his extreme gratitude to personnel in the Boundary Layer Research Branch, particularly Dr J C King (Cardington) and Mr J Crabtree, for arranging and directing the experiment and help in preparing this paper.

References

Businger, J.A. et al, 1971, Flux-profile relationships in the atmospheric surface layer. *J. Atm. Sci.*, 28, 181-189.

Deheer Amissals et al, 1981, Calculation of sensible and latent heat fluxes and surface resistance from profile data. *Boundary-Layer Meteor.*, 20, 35-49.

Dyer, A.J. and B.B. Hicks, 1970, Flux-gradient relationships in the constant flux layer. *Quart. J. Roy. Meteor. Soc.*, 96, 715-721.

Monteith, J.L., 1965, Evaporation and environment. In 'The State and Movement of water in Living Organisms. 19th Symp. Soc. Exp. Biol.', 205-235.

Nielsen, L.B. et al, 1981, Net incoming radiation estimated from hourly global radiation and/or cloud observations. *J. Climatology*, 1, 255-272.

Paulsen, C.A., 1970, The mathematical representation of wind and temperature profiles in the unstable atmospheric surface layer. J. Appl. Meteor., 9, 857-861.

Richards, C.J., 1979, Micrometeorological Characteristics of the 1976 hot spells. Met. Mag., 108, 11-26.

Smith, F.B. and Hunt, R.D., 1978, Estimation of sensible heat flux over grassland. TDN. No. 91.

Wang Jiemin, 1984, Estimation of fluxes from routine meteorological data. (Unpublished).

LIST OF FIGURES

Fig. 1 Daily rainfall during the observational period. The number upon each line denotes the amount of rainfall (mm).

Fig. 2 The experimental site.

RF = Net radiometer (Funk), LYS = Lysimeter

RK = Net radiometer (Kew), G = Soil heat flux plates

Fig. 3 The diurnal variation of soil heat flux at Cardington, 27-28 April 1983.

Fig. 4 Wind profiles in the surface layer on 9-10 May, 1983.

Fig. 5 Diurnal variation of surface energy budget

R = net radiation, E = latent heat flux

H = sensible heat flux, G = soil heat flux

The dotted line denotes the variation of sensible heat flux measured by sonic anemometer.

Fig. 6 A comparison of H calculated by two methods

Mean: $\bar{H}_{\text{profile}} = 52 \text{ W/m}^2$, $\bar{H}_{\text{Residual}} = 80 \text{ W/m}^2$

Standard deviation: $\sigma_{H \text{ profile}} = 76 \text{ W/m}^2$, $\sigma_{H \text{ Residual}} = 80 \text{ W/m}^2$

Correlation: $r = 0.93$

Fig. 7 A comparison of sensible heat flux calculated by the profile method ($H(\text{PROF})$) and measured by sonic anemometer ($H(\text{SS})$, $H(\text{SP})$), where $H(\text{SP})$ is the measured sensible heat flux with temperature measured by platinum wire (denoted by +):

Mean: $\bar{H}_{(\text{ss})} = 23 \text{ W/m}^2$, $\bar{H}_{(\text{prof})} = 40 \text{ W/m}^2$

Standard deviation: $\sigma_{H(\text{ss})} = 42.8 \text{ W/m}^2$, $\sigma_{H(\text{PROF})} = 69.5 \text{ W/m}^2$

Correlation: $r = 0.94$

Fig. 8 A comparison of friction velocity calculated by the profile method ($U^*(PROF)$) and measured by sonic anemometer ($U^*(S)$)

Mean: $\bar{U}^*(S) = 0.30 \text{ m/s}$, $\bar{U}^*(PROF) = 0.34 \text{ m/s}$

Standard deviation: $s_{U^*(S)} = 0.12 \text{ m/s}$, $s_{U^*(PROF)} = 0.16 \text{ m/s}$

Correlation: $r = 0.81$

Fig. 9 Roughness length Z_0 , as a function of wind direction, for each half of the observation period. The mean value for each period is shown in the figure.

Fig. 10 Roughness length Z_0 calculated using wind measurements from different height intervals:

1: 1-3 m

2: 2-8 m

3: 3-16 m

for the data of the first half of observation period.

Fig. 11 The hourly variation of R_n on a typical partly cloudy day, 10 May 1983. The curve is based on the 10 min average of readings taken every 10 sec.

- + Hourly mean value
- o Value calculated by the model

The hourly cloud reports are presented at the top of the diagram. Total amounts are shown in the circle.

Fig. 12 The scatter of R_n with respect to solar elevation s under two cloud conditions:

- Cloud condition I
- + Cloud condition II

$$\text{Curve I: } R_n = 172.1s^3 + 742.2s^2 + 102.5s - 45.0$$

$$\text{Curve II: } R_n = 99.6s^3 + 155.9s^2 + 41.6s + 62$$

Fig. 13 Comparison of observed net radiation (R_{no}) with those calculated by the model (R_{nc})

mean: $R_{no} = 186 \text{ W/m}^2$, $R_{nc} = 197 \text{ W/m}^2$

standard deviation: $R_{RNO} = 148 \text{ W/m}^2$, $R_{RNC} = 147 \text{ W/m}^2$

correlation: $r = 0.92$

standard error: $E = 60 \text{ W/m}^2$

Fig. 14 Comparison of the values of sensible heat flux obtained by the profile method and by the resistance method.

Mean: $H_p = 105 \text{ W/m}^2$, $H_R = 92 \text{ W/m}^2$

Standard deviation: $A_{HP} = 58 \text{ W/m}^2$, $R_{HR} = 48 \text{ W/m}^2$

Correlation: $r = 0.92$

Standard error: $E = 27 \text{ W/m}^2$

Fig. 15 Comparison of the values of friction velocity obtained by the profile method and by the resistance method.

Mean: $U^*_p = 0.40 \text{ m/s}$, $U^*_R = 0.38 \text{ m/s}$

Standard deviation: $R_{U^*_p} = 0.14 \text{ m/s}$, $R_{U^*_R} = 0.12 \text{ m/s}$

Correlation: $= 0.95$

Standard error: $E = 0.05 \text{ m/s}$

Appendix: Data Tabulation

The data tabulated are mainly hourly mean values which were selected from the whole data set according to the following criteria:

- a. No rainfall during the hour;
- b. No identifiable instrument malfunction (some data apparently wrong are printed with *****)

The first part of the data consist of:

WD	= Wind direction (16 m), deg from true N	Porton type wind vane and anemometers
U1	= Wind speed (1 m), ms^{-1}	
U2	= Wind speed (3 m), ms^{-1}	
U3	= Wind speed (8.7 m), ms^{-1}	
U4	= Wind speed (16 m), ms^{-1}	
RNF	= Net radiation, measured by Funk type radiometer, Wm^{-2}	
RNK	= Net radiation, measured by Kew type radiometer, Wm^{-2}	
G5R	= Soil heat flux at 5 cm, reference, Wm^{-2}	
G5	= Soil heat flux at 5 cm, Wm^{-2}	
G10	= Soil heat flux at 10 cm, Wm^{-2}	
G15	= Soil heat flux at 15 cm, Wm^{-2}	
G	= Surface soil heat flux, Wm^{-2}	
LE	= Latent heat flux, Lysimeter, Wm^{-2}	
USON	= Mean Wind speed measured by sonic anemometer at 16 m, ms^{-1}	
Tp	= Temperature, measured by platinum wire, at 16 m, $^{\circ}\text{C}$.	
HS	= Sensible heat flux, measured by sonic anemometer, Wm^{-2}	

$$\begin{aligned}
 HP &= \text{Sensible heat flux, measured by platinum wire + sonic, } \text{Wm}^{-2} \\
 UW &= \overline{U'W'} = -U_*^2 \\
 UU &= \overline{U'U'} \\
 VV &= \overline{V'V'} \\
 WW &= \overline{W'W'}
 \end{aligned}
 \left. \begin{array}{l} \\ \\ \end{array} \right\} \text{measured by sonic anemometer, M}^2\text{S}^{-2}$$

The second part of the data consist of:

T = temperature, screen (1.15 m) dry bulb, $^{\circ}\text{C}$

h = relative humidity, screen (1.15 m), %

cloud, including cloud condition (I or II), total amount, main type and its amount. The cloud condition was grouped mostly according to the pictures of sky camera (Cardington); some were from Bedford data.

Time: Julian day number had been used, see table below.*

H~GMT.

*Table: The date and Julian day number

Date	Julian	Date	Julian
Apr 22	112	May 6	126
23	113	7	127
24	114	8	128
25	115	9	129
26	116	10	130
27	117	11	131
28	118	12	132
29	119	13	133
30	120	14	134
May 1	121	15	135
2	122	16	136
3	123	17	137
4	124	18	138
5	125		

APPENDIX

Day/H	T°C	h%	Cloud	Day/H	T°C	h%	Cloud
112 9	10	77	II 7/1Cu5Sc7Ac	115 16	12	58	II 7/2Cu6Sc
: 10	10	75	II 7/2Cu4Sc7Ac	: 17	12	62	II 7/1Cu7Sc
: 11	11	75	II 7/3Cu3Sc6Ac	: 18	12	63	II 6/1Cu5Ci
: 12	13	70	I 5/4Cu	: 19	11	74	II 7/1Cu4Sc5Ci
: 13	12	72	II 6/6Cu	116 7	8	88	I 2/1Sc
: 15	12	76	II 6/4Cb	: 8	11	85	I 3/2Sc3Ci
: 16	14	67	II 6/3Cb3Sc	: 9	13	79	I 3/1Sc3Ci
113 7	9	90	I 1/1Sc	: 10	14	68	I 4/1Cu4Ci
: 8	11	84	I 4/4Cu	: 11	16	63	I 5/3Cu3Ci
: 9	11	77	I 7/2Cu6Ci	: 17	11	90	II 7/6Cb3Ac5Ci
: 10	11	71	I 7/3Cu7Ci	: 18	11	88	II 7/2Cb3Sc6Ci
: 11	12	69	I 7/6Cu7Cs	: 19	10	95	II 6/1Cb5Ac
: 12	13	66	I 7/4Cu7Cs	117 7	8	99	II 7/4St6Sc
: 13	13	62	I 6/3Cu7Cs	: 8	8	96	II 8/8St
: 14	12	58	I 6/5Cu3Ci	: 9	9	95	II 8/8St
: 15	14	56	I 6/3Cu4Ci	: 10	11	87	I 7/2Cu7Cs
: 16	14	66	II 7/3Cu7Sc	: 11	12	81	I 7/2Cu7Cs
: 18	12	96	II 6/1Cb4Sc	: 12	13	78	II 7/1Cu7Cs
: 19	10	96	II 7/6Cb	: 13	13	74	I 7/1Cu7Cs
114 7	9	95	I 3/1Cu3Sc	: 14	14	70	I 7/1Cu7Cs
: 8	10	86	I 1/1Cu	: 15	13	69	I 7/1Cu7Cs
: 9	11	78	I 3/2Cu	: 16	13	64	I 7/1Cu7Cs
: 10	12	66	I 5/5Cu	: 17	12	66	I 7/1Cu7Sc
: 12	13	62	I 7/2Cu7Cs	: 18	10	85	I 7/1Cu7Cs
: 13	13	61	II 7/2Cu4Ac	: 19	9	93	I 7/1Ac7Cs
: 14	12	58	I 6/2Cu5Ci	118 10	12	83	II 7/3St7Sc
: 15	14	58	I 7/3Cu6Cs	: 11	13	80	I 5/Cu
: 16	14	70	I 6/2Cu5Ci	: 12	13	79	I 5/5Cu
: 17	13	76	I 1/1Cu	: 13	14	74	I 4/4Cu
: 18	12	96	I 3/1Cu3Ci	: 14	15	70	I 6/4Cu4Ci
: 19	10	96	I 5/1Ac5Ci	: 15	15	56	I 4/4Cu
115 8	8	95	II 8/8Sc	: 16	15	60	I 4/4Cu
: 9	8	93	I 8/1St6Sc8Ac	: 17	14	61	I 2/2Cu
: 10	10	93	I 7/1St4Cu7Ac	: 18	12	58	I 5/1Cb
: 11	11	75	I 5/5Cu	: 19	11	71	I 6/5Cu
: 12	13	63	I 6/6Cu	119 7	8	87	I 8/3Sc6Ac8Cs
: 13	13	63	I 5/4Cu	: 8	10	94	I 2/1St
: 14	13	61	II 6/5Cu	: 9	12	82	I 2/1Cu
: 15	13	59	II 7/3Cu6Sc	: 10	14	74	I 3/3Cu

Day/H	T°C	h%	Cloud	Day/H	T°C	h%	Cloud
123 9	9	82	II 7/4Cu7Sc	126 15	12	64	I 6/5Cu
: 10	9	77	II 7/3Cu7Sc	: 16	12	63	I 3/1Cu3Sc
: 11	10	73	II 8/3Cu8Sc	: 17	11	66	I 2/1Cu
: 12	11	68	II 7/3Cu5Sc	129 12	12	88	II 8/5St8Sc
: 13	11	67	II 8/3Cu8Sc	: 13	12	79	I 8/1Cu8Sc
: 14	11	67	II 8/4Cu5Sc	: 14	13	69	I 5/3Cu
: 15	12	62	II 7/3Cu7Sc	: 15	13	62	I 7/5Cu
: 17	11	73	II 6/3Cu5Sc	: 16	13	62	I 7/6Cu
: 19	10	86	I 4/3Cu3Sc	: 17	12	57	I 6/3Ac
124 7	5	100	II FOG	: 18	10	56	I 4/4Cu
: 8	6	100	II FOG	: 19	8	59	4/4Cu
: 9	7	100	I 8/8St	130 7	7	83	I 7/1Cu7Cs
: 10	9	98	I 8/7St	: 8	9	78	I 7/1Cu6Cs
: 11	11	88	I 6/6St	: 9	10	68	I 7/5Cb5Cs
: 12	12	87	I 5/5Cu	: 10	11	63	I 6/5Cu
: 13	13	71	I 2/2Cu	: 11	12	60	I 6/5Cu
: 14	14	69	II 2/2Cu	: 12	12	58	I 6/5Cu
: 15	13	64	II 3/3Cu	: 13	12	60	I 6/1Cb4Cn
: 16	13	70	II 6/2Cu5Sc	: 14	13	61	I 5/1Cb5Cu
: 17	12	74	I 8/2Cu8Sc	: 15	12	60	I 6/2Cb5Cu
: 18	11	76	8/8Sc	: 16	12	64	I 6/1Cb4Cu
: 19	11	82	8/8Sc	: 17	11	64	I 7/1Cb3Cu
125 7	10	95	I 8/7St6Sc	: 18	10	66	I 7/1Cu6Ci
: 8	12	93	I 8/6St8Sc	: 19	9	68	I 7/1Cu6Cs
: 9	14	87	I 7/3St6Cs	131 7	7	90	I 5/2St4Cu
: 10	15	82	I 7/1St3Sc7Cs	: 8	9	82	I 7/2St5Cu
: 11	16	78	II 7/1Cu3Ac7Cc	: 9	10	72	I 7/4Cu2Sc
: 12	16	75	II 8/4Cu8Cs	: 10	11	69	II 7/7Cu
: 13	17	74	II 8/4Cu4As8Cs	: 11	11	65	II 8/4Cu3Sc
: 14	17	73	II 8/4Cu8As	: 12	11	64	II 7/5Cu6Sc
: 15	17	72	II 8/3Sc8As	: 13	13	57	I 6/3Cu3Sc
: 16	16	77	I 8/3Sc8As	: 14	12	60	II 7/7Cu
: 17	16	75	I 8/1Sc3Ac8Cs	: 15	12	67	I 7/7Cu
126 9	14	98	II 7/4St7Sc	: 16	11	76	I 6/3Cu4Sc
: 10	11	87	II 7/2St6Cu6Sc	: 17	11	76	I 5/2Cu3Sc
: 11	12	76	I 5/5Cu	: 18	11	79	I 5/5Cu
: 12	12	71	I 5/5Cu	: 19	9	85	I 3/3Cu
: 13	12	70	I 6/3Cu3Sc	132 10	9	90	8/2St5Sc8Ns
: 14	12	68	I 6/4Cu3Sc	: 11	10	82	II 7/6Cu7Sc

Day/H	T°C	h%	Cloud	Day/H	T°C	h%	Cloud
132 12	12	73	I 7/3Cu6Sc	137 14	13	74	I 7/1cb4Cu5Sc
: 13	12	80	I 5/5Cu	: 15	13	74	I 7/3Cb5Sc
: 14	13	70	I 4/4Cu	: 16	13	74	I 6/1cb3Cu
: 17	10	84	7/6Cb	: 17	12	80	I 6/2Cu3Sc
134 7	9	92	I 7/2St7Sc	: 18	11	83	I 6/2Cb3Sc
: 8	10	80	I 6/6Cu	: 19	10	86	I 6/1Cb5Cu
: 9	11	76	I 6/6Cu				
: 10	12	67	I 6/6Cu				
: 11	14	60	I 6/6Cu				
: 12	15	56	II 6/1Cb5Cu				
: 13	15	57	II 7/2Cb4Cu				
: 14	15	51	I 6/2Cb4Cu				
: 5	15	48	I 5/1Cb4Cu				
: 16	14	62	I 5/1Cb4Cu				
: 17	14	63	I 4/1Cb3Cu				
: 18	14	61	I 4/1Cb3Cu				
: 19	12.	62	I 4/2Cu3Ci				
135 13	10	90	II 7/1Cu7Ns				
: 14	10	90	I 8/1St7As8Cs				
: 15	12	86	I 7/3Cu6Cs				
: 16	13	71	I 7/2Cu3Sc6Ci				
: 17	14	61	I 4/3Cu				
: 18	13	57	I 1/1Cu				
: 19	12	67	I 1/1Cu				
136 7	11	80	I 7/2Ac7Ci				
: 10	17	70	I 7/1Cu7Ci				
: 11	17	62	I 7/4Cu6Ci				
: 12	17	61	I 7/3Cu6Ci				
: 13	17	61	II 7/3Cu6Cs				
: 17	12	96	7/1St7Sc				
: 18	12	96	7/1Cu5Ac5Ci				
: 19	11	96	7/1St7Ac				
137 7	11	84	I 4/4Cu				
: 8	12	80	I 6/6Cu				
: 9	13	74	II 7/5Cu3Sc				
: 10	13	70	II 71St6Cu				
: 11	14	70	II 7/5Cu5Sc				
: 12	15	65	I 7/1Cu6Sc				
: 13	14	65	I 7/5Cu4Sc				

DATA OF EXPERIMENT OF SURFACE ENERGY BALANCE, CARDINGTON APRIL MAY 1983. HOURLY MEANS
U₂ U₃ U₄ U₅ DT₁ DT₂ R₁ R₂ R₃ R₄ R₅ R₆ USON TB

DATA OF EXPERIMENT OF SURFACE ENERGY BALANCE, CARDINGTON APRIL, 1983. HOURLY MEANS

DATA OF EXPERIMENT OF SURFACE ENERGY BALANCE CARDINGTON APRIL 1983. HOURLY MEANS
 U2 DT1 DT2 RNF RNC GFR G15 G16 LE USON TP

Fig 1

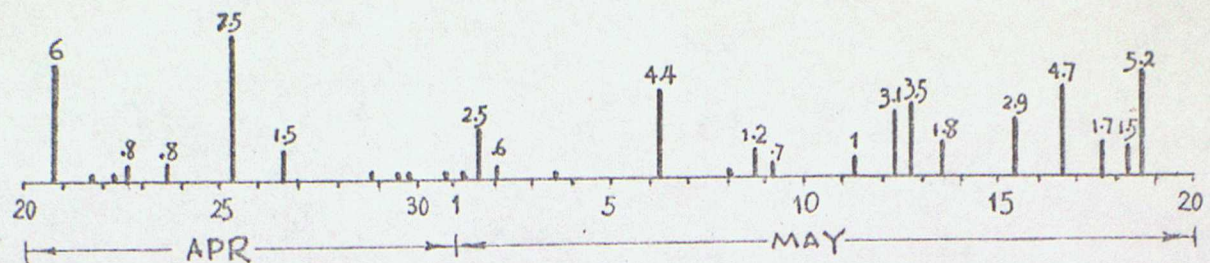
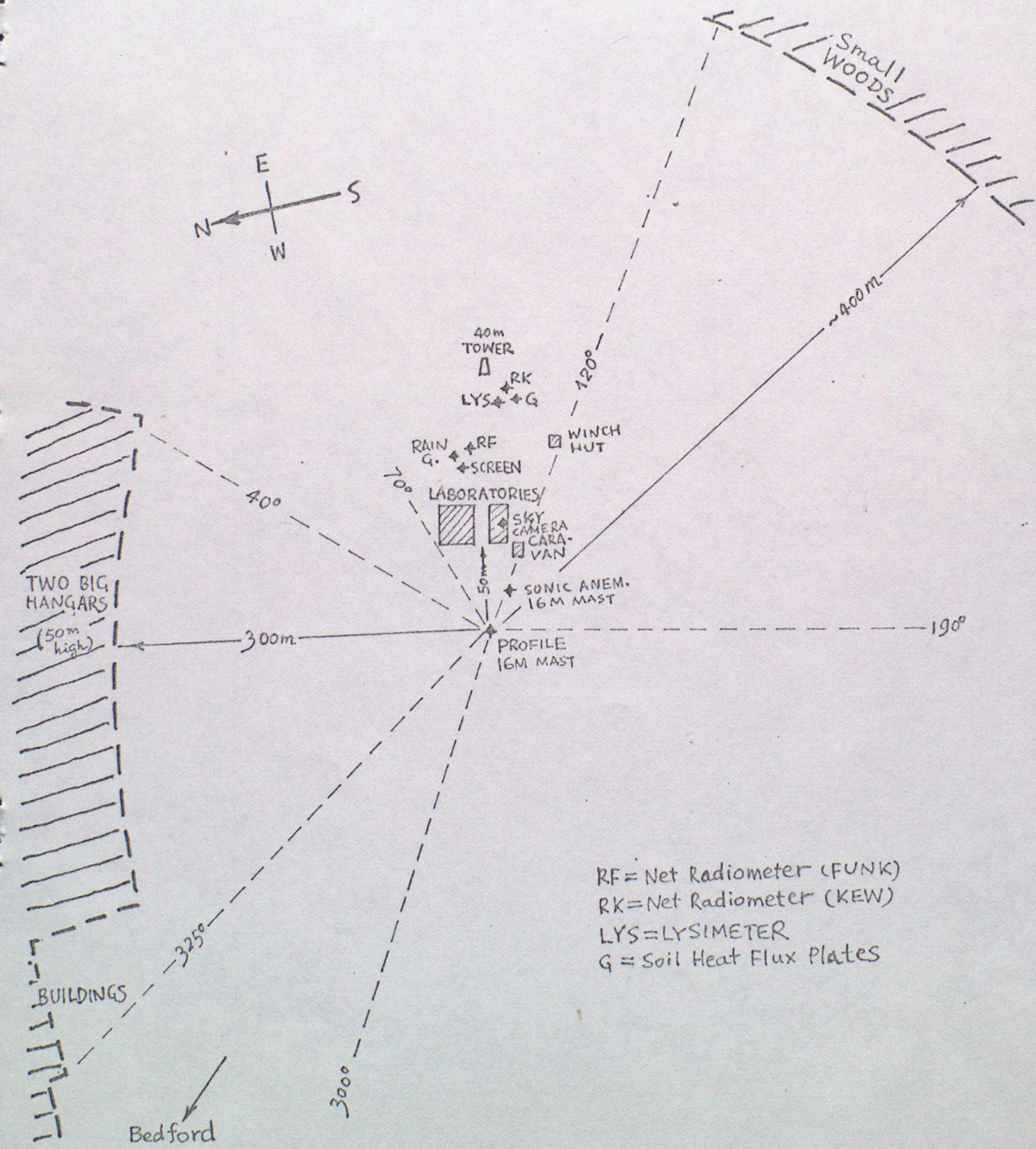


Fig 2



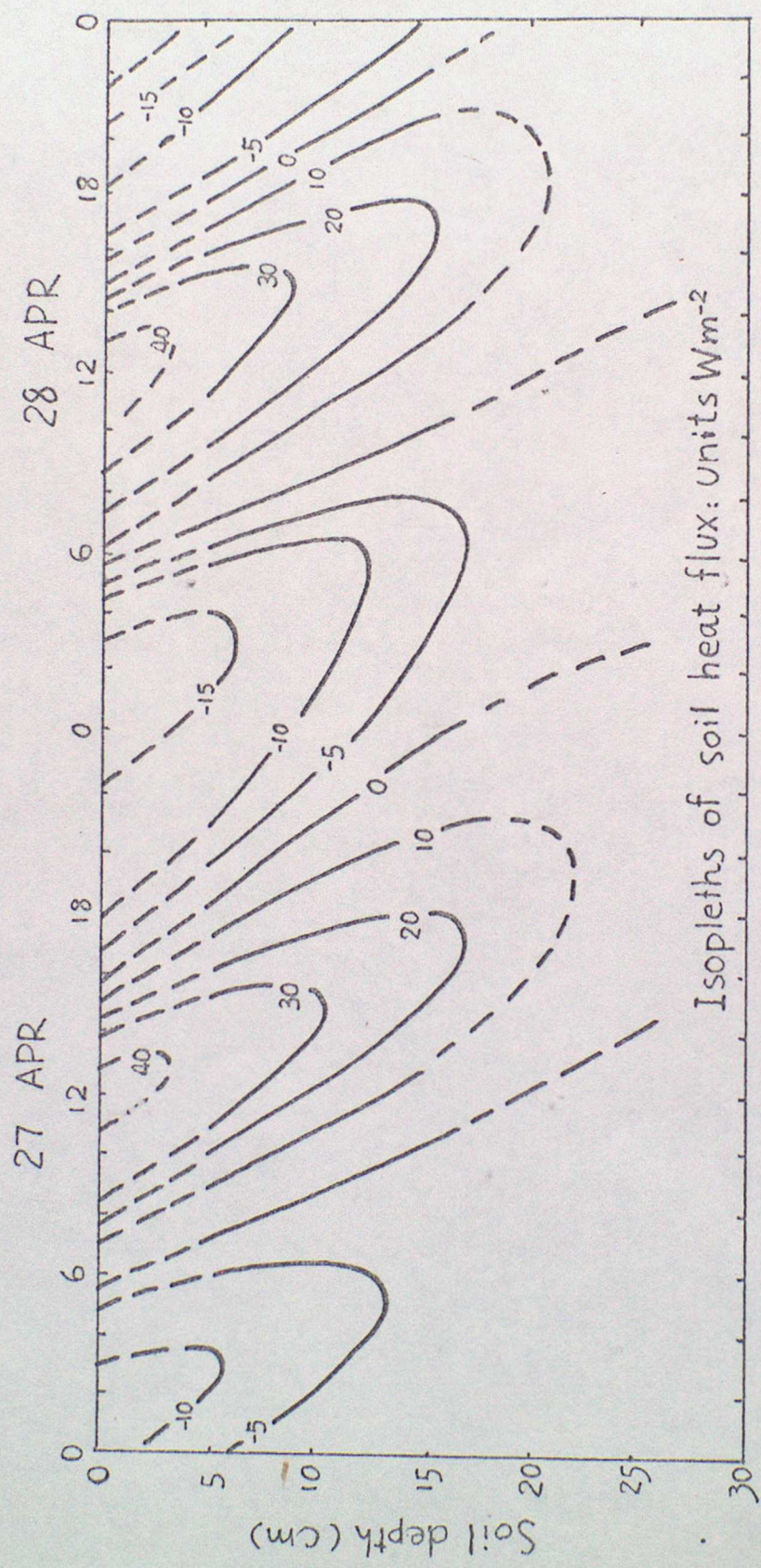


Fig 3 . The diurnal variation of Soil heat flux
at Cardington: 27-28 Apr. 1983

WIND PROFILES 9-10.MAY.1983
THE NUMBERS BELOW EACH LINE ARE HOURS

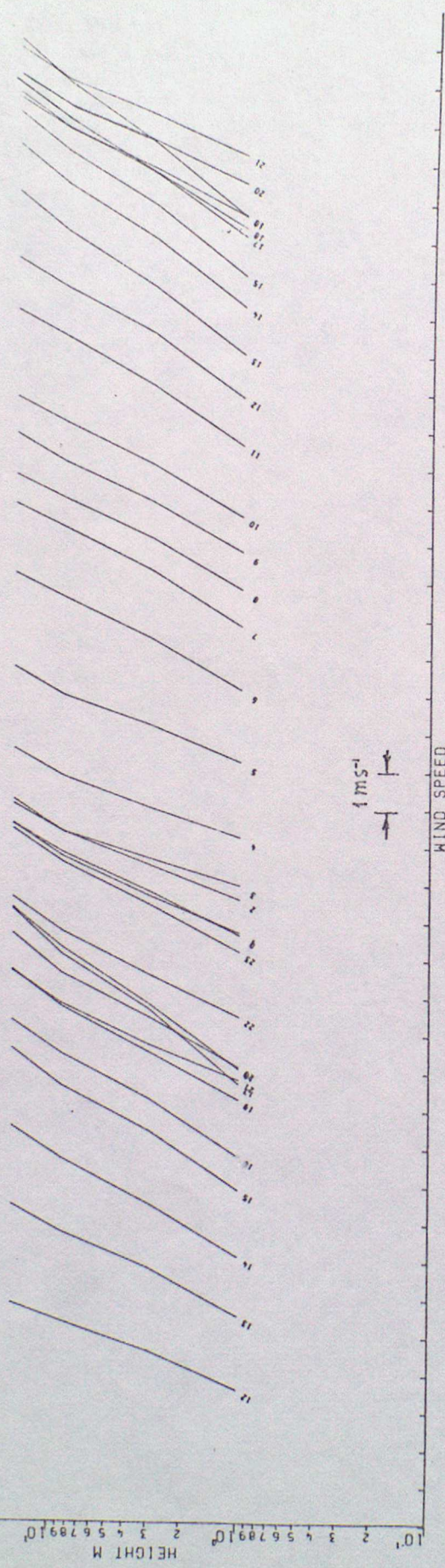


Fig. 4. Wind Profiles in the surface layer on 9-10, May, 1983.

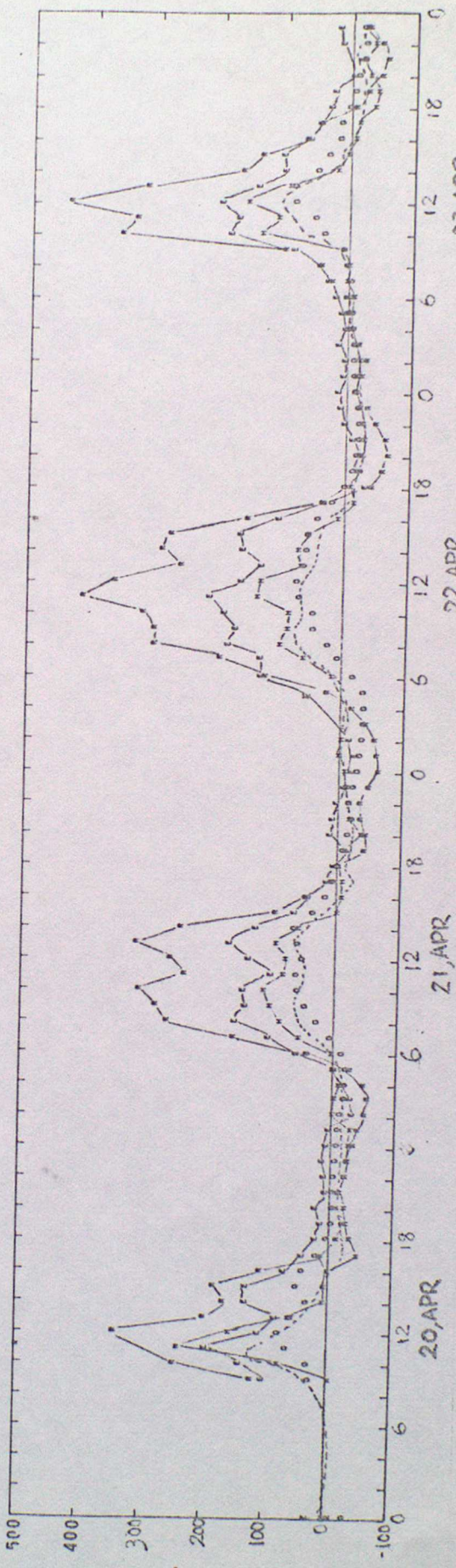


Fig. 5. Diurnal variation of surface energy budget.
R = net Radiation, E = Latent heat flux,
H = Sensible heat flux, G = Soil heat flux.

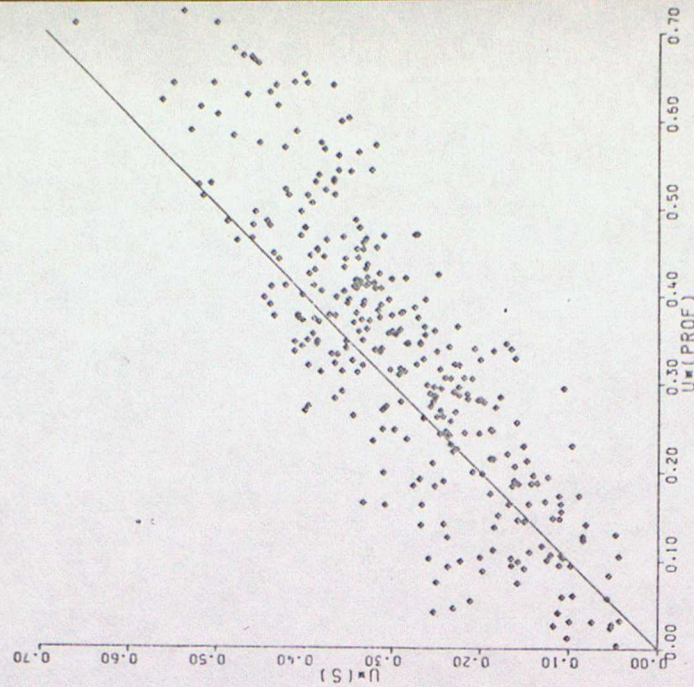


Fig 8

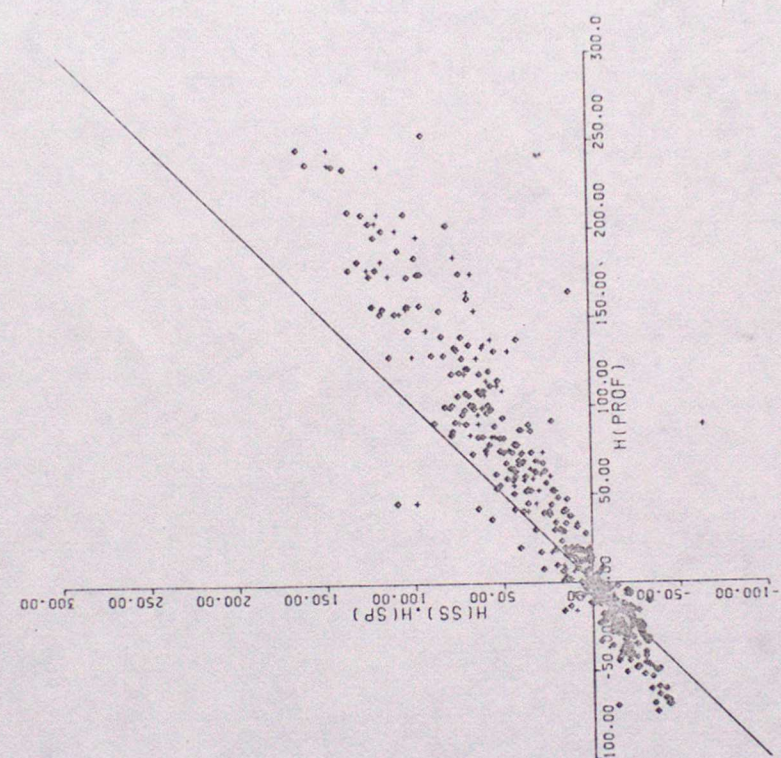


Fig 7

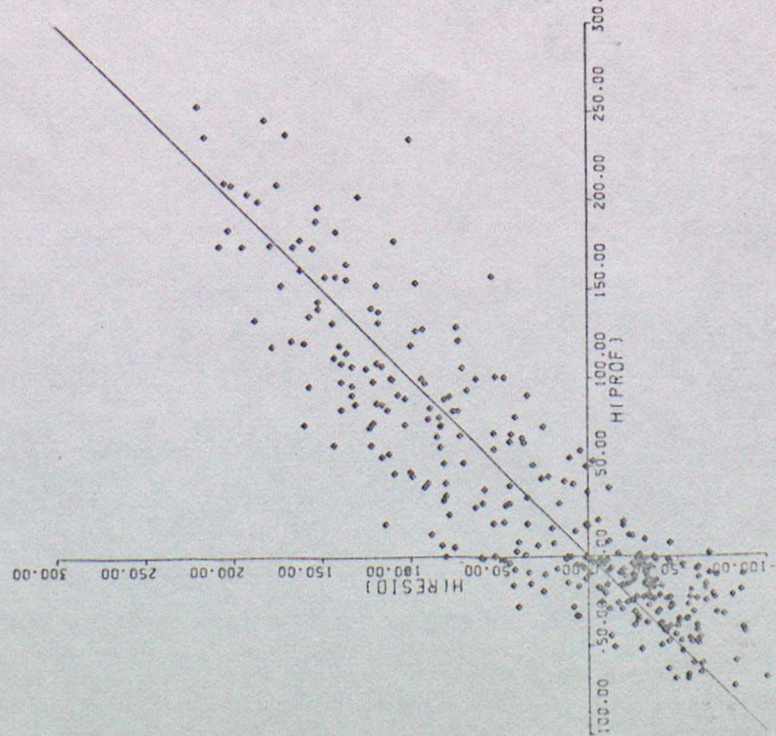


Fig 6

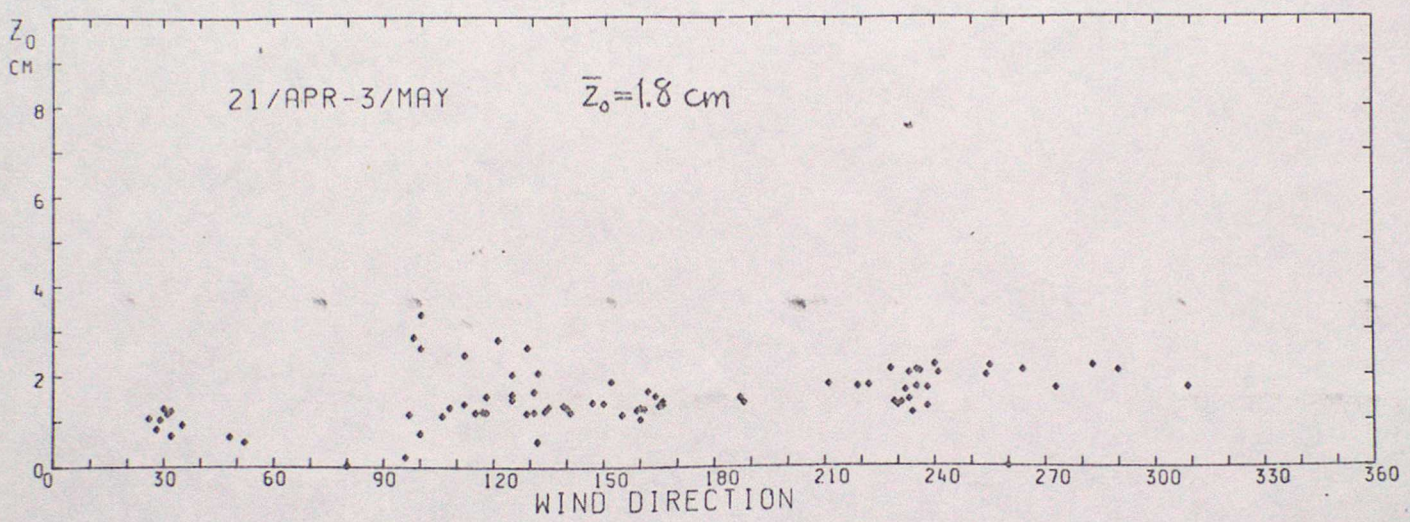
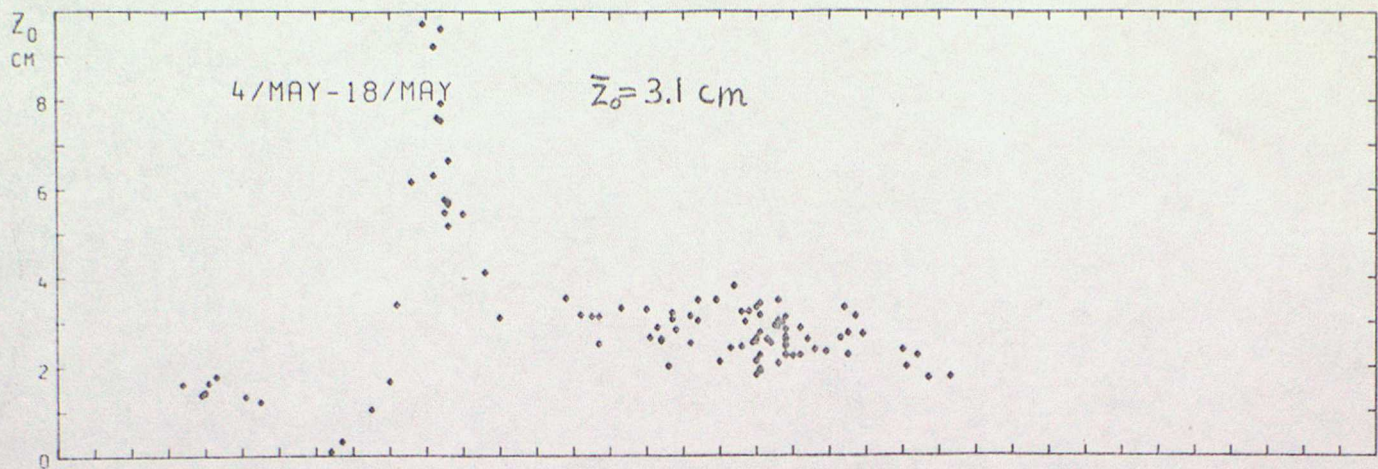


Fig 9

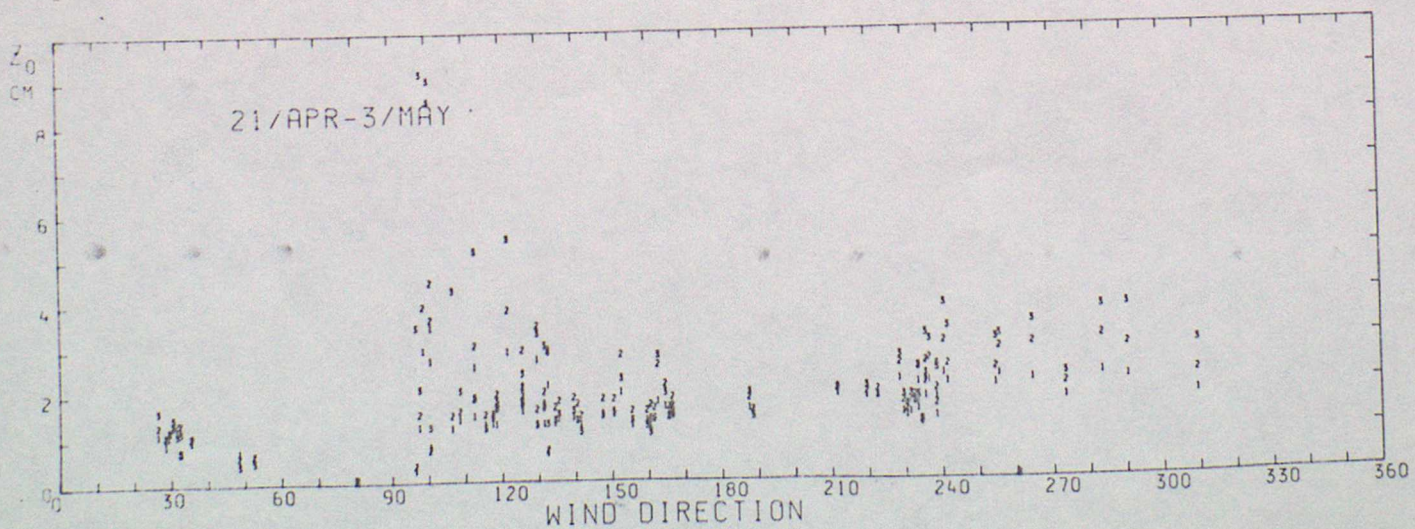


Fig 10

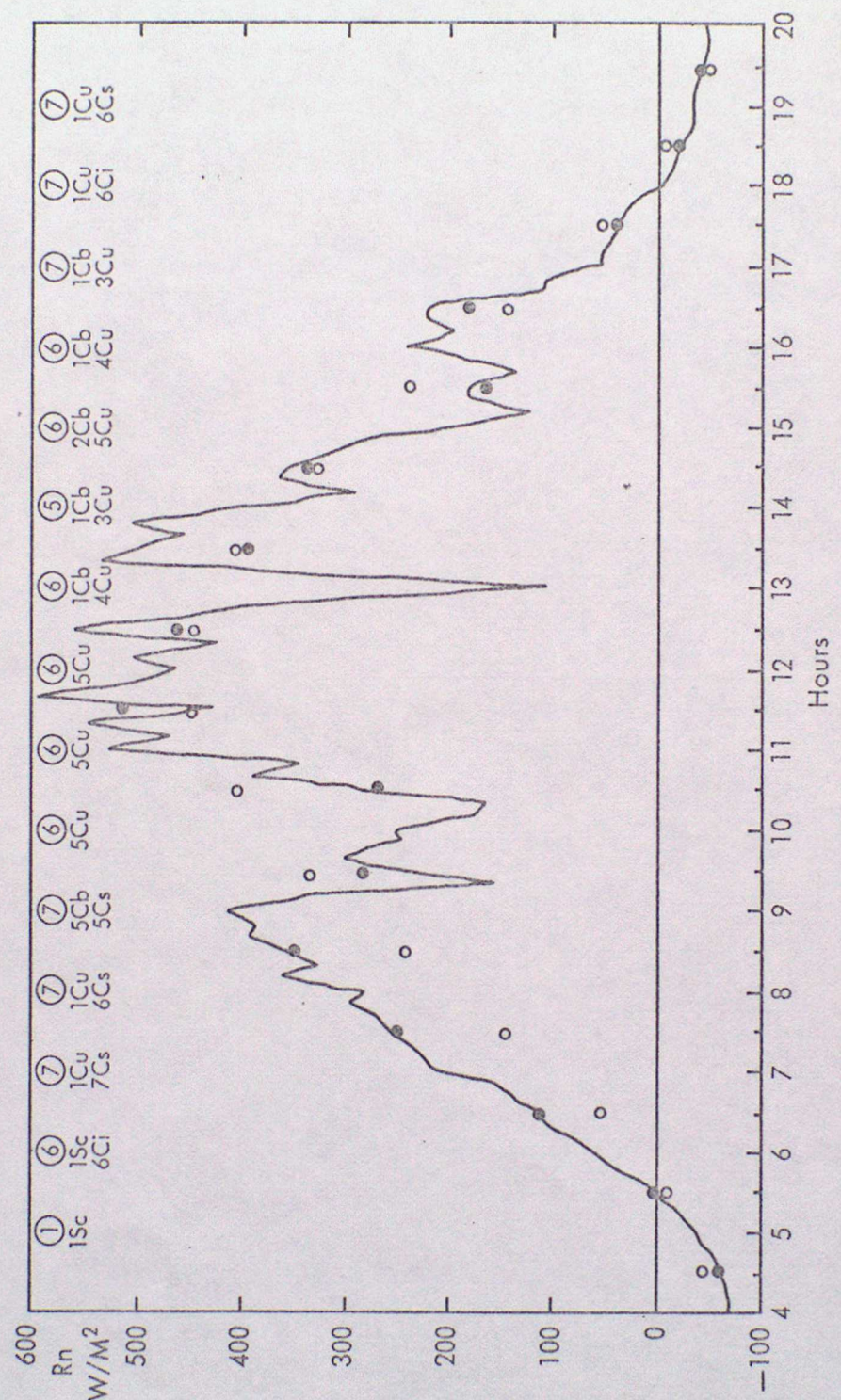


Fig 11

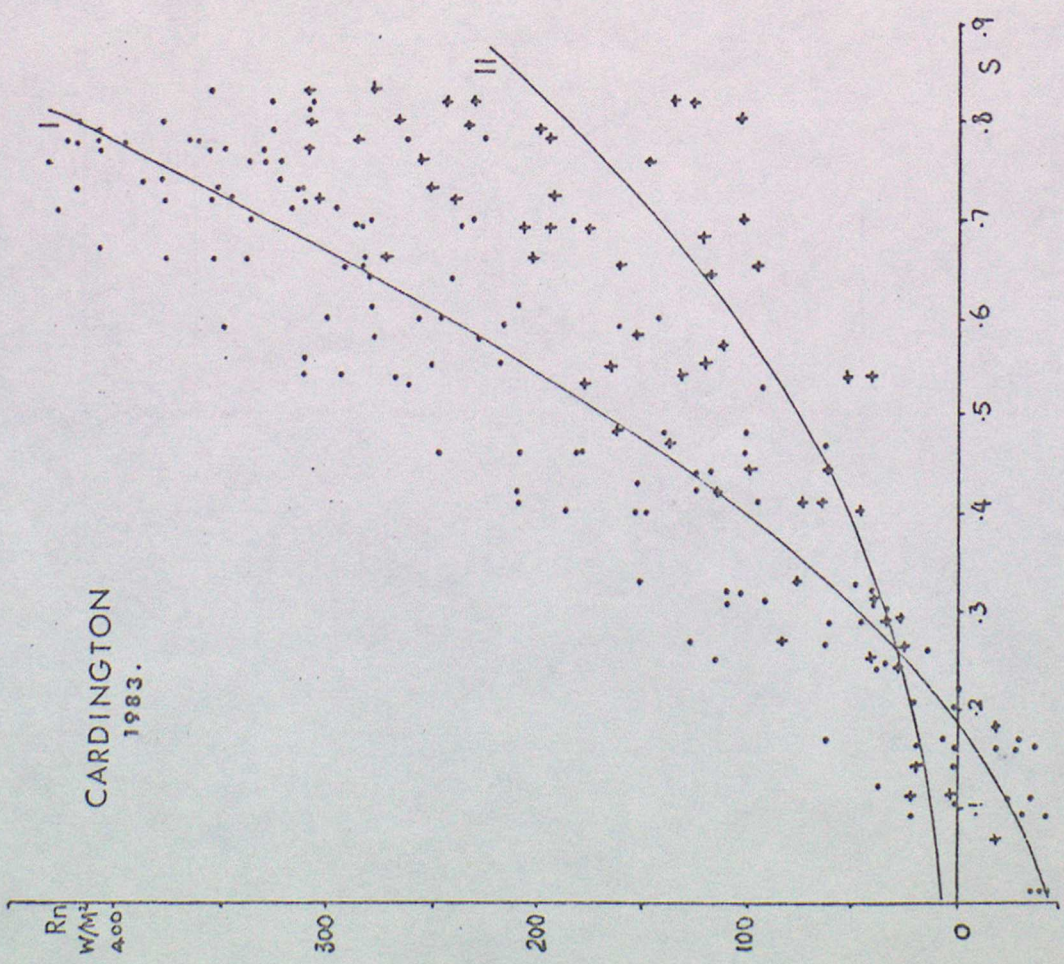
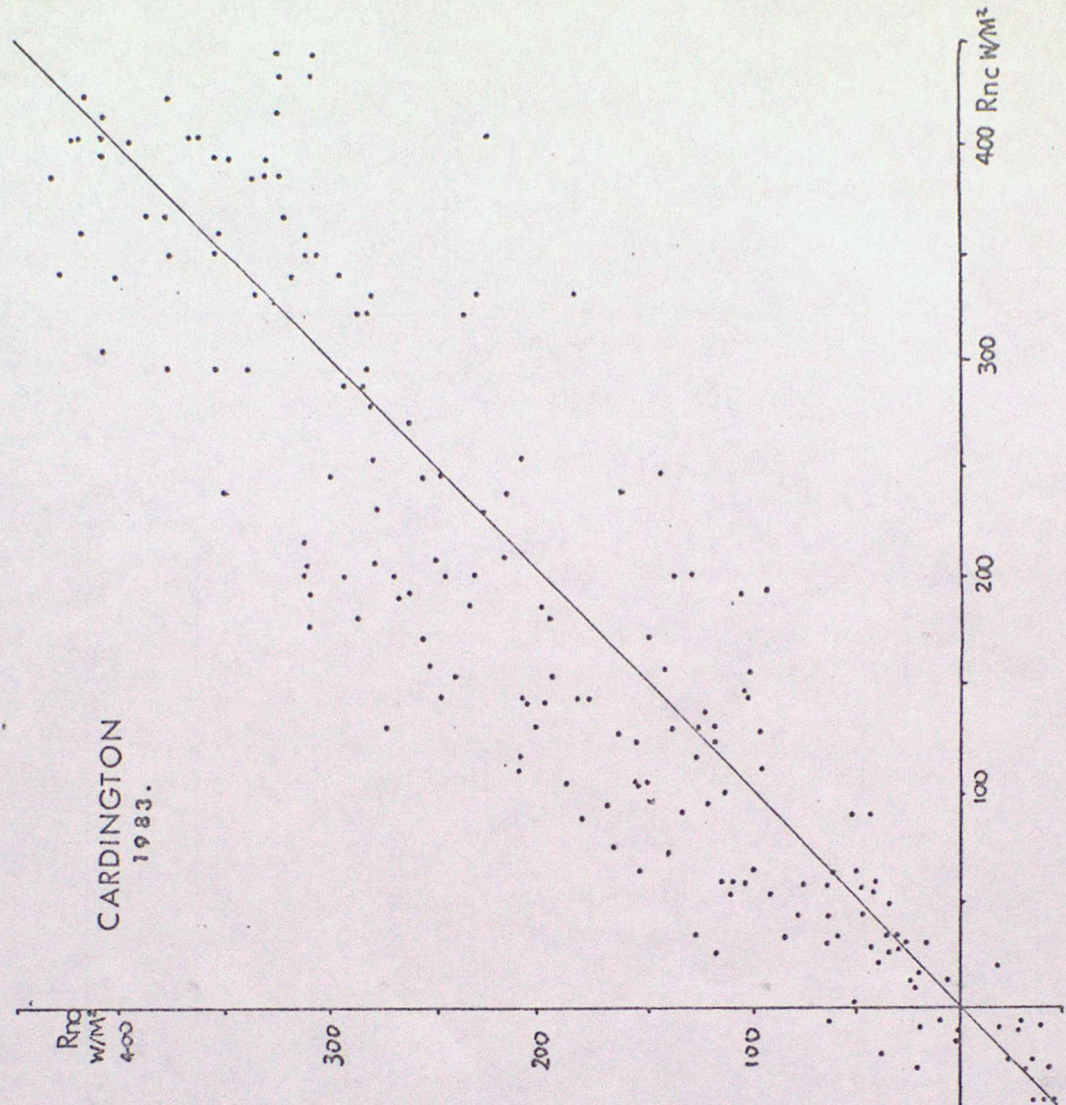


Fig. 12

Fig. 13

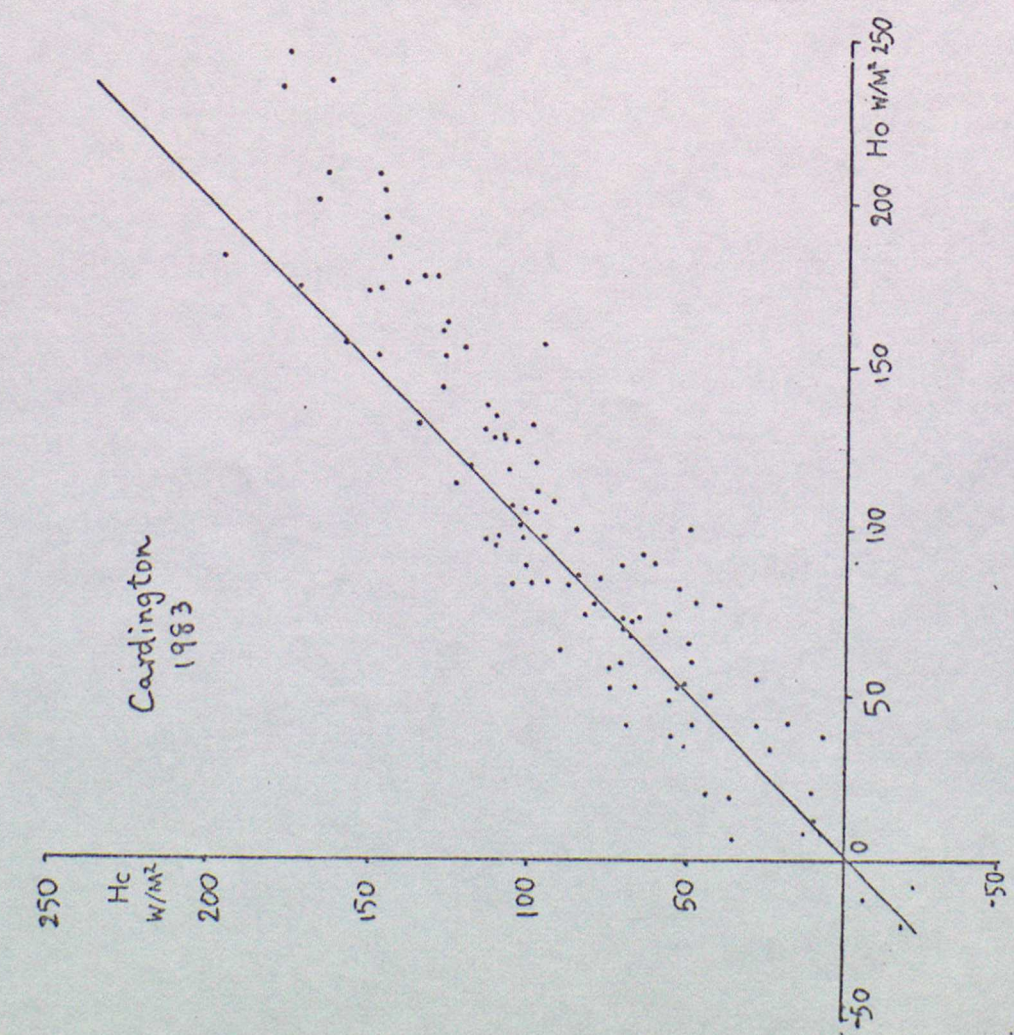


Fig 14

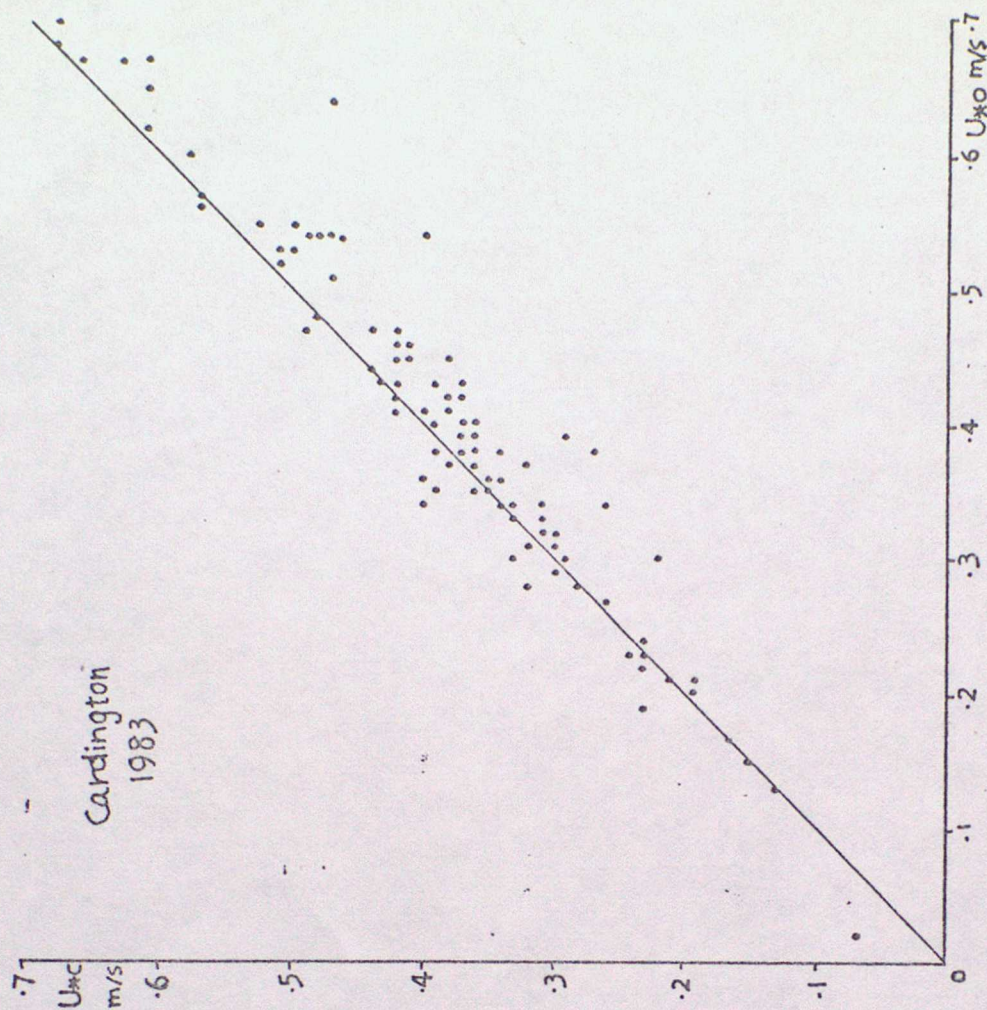


Fig 15